

Document downloaded from:

<http://hdl.handle.net/10251/80798>

This paper must be cited as:

Desantes Fernández, JM.; López, JJ.; Molina, S.; López Pintor, D. (2016). Theoretical development of a new procedure to predict ignition delays under transient thermodynamic conditions and validation using a Rapid Compression-Expansion Machine. *Energy Conversion and Management*. 108:132-143. doi:10.1016/j.enconman.2015.10.077.



The final publication is available at

<https://doi.org/10.1016/j.enconman.2015.10.077>

Copyright Elsevier

Additional Information

Theoretical development of a new procedure to predict ignition delays under transient thermodynamic conditions and validation using a Rapid Compression-Expansion Machine

José M. Desantes, J. Javier López*, Santiago Molina, Darío López-Pintor

*CMT-Motores Térmicos
Universitat Politècnica de València
Camino de Vera, s/n. 46022 Valencia, SPAIN*

Abstract

An experimental and theoretical study about the autoignition phenomenon has been performed in this article. A new procedure to predict ignition delays under transient (i. e. variable) thermodynamic conditions has been developed starting from the Müller's chemical kinetics mechanism. The results obtained have been compared with those obtained from the Livengood & Wu integral method, as well as with direct chemical kinetic simulations. All simulations have been performed with CHEMKIN, employing a detailed chemical kinetic mechanism. The simulations have been validated in the working range versus experimental results obtained from a Rapid Compression-Expansion Machine (RCEM). The study has been carried out with n-heptane as a diesel fuel surrogate. The experimental results show a good agreement with the direct chemical kinetic simulations. Besides, better predictions of the ignition

*Corresponding author

Tel: +34 963 879 232. Fax: +34 963 877 659. E-mail: jolosan3@mot.upv.es

delay have been obtained from the new procedure than the ones obtained from the classic Livengood & Wu expression.

Keywords: RCEM, ignition delay, autoignition modeling, CHEMKIN

1 **1. Introduction, justification and objective**

2 The potential of new combustion modes, such as Homogeneous Charge
3 Compression Ignition (HCCI), Premixed Charge Compression Ignition (PCCI)
4 and others based on Low Temperature Combustion (LTC), for the simulta-
5 neous reduction of soot and NO_x has been widely proved in previous studies
6 [1, 2]. These modes show virtually zero emissions of soot and NO_x , but high
7 emissions of unburned hydrocarbons (UHC) and carbon monoxide (CO),
8 by avoiding the soot and NO_x formation peninsulas, which can be seen in
9 equivalence ratio - temperature diagrams [3]. The lack of control over the
10 autoignition process and over the heat release rate are the main challenge
11 to implement these new combustion strategies in commercial reciprocating
12 internal combustion engines [4].

13 The ignition control is much more difficult under these conditions because
14 of the absence of a explicit ignition-controlling event, such as a spark or an
15 injection process when very reactive conditions are reached in the combus-
16 tion chamber (near top dead center). Thus, the ignition is controlled by the
17 chemical kinetics of the charge [5], which can be modified by adjusting the
18 engine operating parameters, such as the Exhaust Gas Recirculation (EGR)
19 rate and the inlet temperature. Therefore, it is necessary to improve the ca-
20 pability of predicting the autoignition event to properly modify the operating
21 conditions of the engine and control the heat release.

22 Although ignition can be reasonably predicted by using advanced CFD
23 codes with detailed chemistry, the required computing time is too long to
24 be solved in real time. In fact, simple numerical methods with very short
25 computing time are the only ones that can be implemented in an engine
26 control unit. Low computing time methods with enough accuracy to predict
27 ignition delays allow improving the control of the engine, since decisions in
28 real time can be taken.

29 The Livengood & Wu hypothesis [6], also known as the Livengood & Wu
30 integral or, simply, the integral method, allows obtaining ignition delays of
31 processes under transient conditions of temperature and pressure by using the
32 ignition characteristics under constant thermodynamic conditions, which are
33 much easier to obtain both experimentally and by simulation. The expression
34 proposed by these authors is the following:

$$\int_0^{t_i} \frac{1}{\tau} dt = 1 \quad (1)$$

35 where t_i is the ignition delay of the process and τ is the ignition delay under
36 constant conditions of pressure and temperature for the successive thermo-
37 dynamic states.

38 The Livengood & Wu integral assumes that the oxidation process during
39 the ignition delay can be described by a single zero-order global reaction and,
40 therefore, the reaction rate does not depend on time under constant thermo-
41 dynamic conditions. The negative temperature coefficient (NTC) behavior
42 cannot be modeled under this hypothesis. Moreover, the authors assumed
43 that the autoignition happens when a critical concentration of chain carri-
44 ers is reached, being this critical concentration constant with pressure and

45 temperature for a given air-fuel mixture.

46 Whereas this integral has been traditionally enunciated as a method to
47 predict the occurrence of knock in SI-engines [7], it has been extended to
48 CI-engines as a way to predict the ignition delay of homogeneous air-fuel
49 mixtures as the ones used in HCCI engines [8]. A new use of the Livengood
50 & Wu integral is its implementation in an engine control unit. Several authors
51 such as Ohyama [9], Rausen et al. [10], Choi et al. [11] and Hillion et al.
52 [12] used the integral method to predict the start of combustion under HCCI
53 conditions. This method can be combined with other simple models to obtain
54 global parameters of the combustion process allowing the control of the engine
55 in real time. The integral method has great interest for the prediction of
56 autoignition due to its simplicity and low computational cost. This simplicity
57 is just a consequence of the hypotheses assumed for its development.

58 The validity of the Livengood & Wu integral under certain conditions has
59 been wondered by several authors [13]. When a two-stage ignition occurs, the
60 integral method is not able to accurately predict any of both delays because
61 it is based on a single global reaction mechanism that ignores the cool flames.
62 Some of these authors, as Liang and Reitz [14] or Edenhofer et al. [15], show
63 the need to create simple algorithms, but more sophisticated than the integral
64 method, to characterize the autoignition at low temperatures without using
65 any chemical kinetic mechanism. However, few alternatives to the Livengood
66 & Wu integral can be found in the literature.

67 Hernandez et al. [16] analyzed the validity of the Livengood & Wu in-
68 tegral by simulations performed with CHEMKIN for several fuels and with
69 various chemical kinetics mechanisms. They proved that the predictions of

70 the method are accurate if the fuel do not show a two-stage ignition pat-
71 tern. These authors also proposed two different alternatives, one with better
72 and another with worse results than the integral method. However, most of
73 the alternatives proposed to improve the integral method are based on the
74 method itself or assume the same hypotheses, which are too simple. Expres-
75 sions based on more sophisticated autoignition models are needed in order
76 to extend the range of validity of the methods.

77 In this study the validity of an alternative procedure to determine ignition
78 delays under transient conditions is intended to be solved. The study has
79 been done with n-heptane, the reactivity of which is very similar to diesel
80 fuel. Despite the fact that more sophisticated surrogate fuels for diesel can
81 be found in the literature, n-heptane was chosen because extended and fully
82 validated chemical kinetic mechanisms are available for it. Moreover, n-
83 heptane is a primary reference fuel (PRF) employed to define the octane
84 reference scale and it is widely used in the literature as a diesel fuel surrogate
85 under engine conditions [17].

86 Ignition delays and critical concentrations for n-heptane will be obtained
87 under different conditions of pressure, temperature, equivalence ratio and
88 oxygen mass fraction from calculations performed with the software of chem-
89 ical simulation CHEMKIN. This software, which is developed by Reaction
90 Design (ANSYS), is consolidated in the world of engineering investigations
91 and the chemical kinetics mechanisms of several hydrocarbons are perfectly
92 defined to be used with it. Finally, the numerical results are validated ex-
93 perimentally using a Rapid Compression-Expansion Machine (RCEM).

94 The structure of the paper is as follows: first, the experimental facili-

95 ties involved in the study are presented. Then, a new expression to predict
96 ignition delays under transient conditions is theoretically developed. After-
97 ward, the methodological approach is described, including the experimental
98 methods, the chemical kinetic simulations, the predictive methods and the
99 parametric study performed. Next, the chemical kinetic mechanism is val-
100 idated by comparison with experimental results. Thereafter, the predictive
101 methods are validated with the chemical simulations, since they cannot be
102 compared with the experiments due to they are referred to a different stage
103 of the autoignition process. Finally, the conclusions of this study are shown.

104 **2. Experimental facilities**

105 A RCEM is an experimental facility widely used in autoignition studies
106 due to its capability to reproduce engine conditions [18]. It allows a detailed
107 analysis of a single engine cycle of an internal combustion engine, includ-
108 ing not only the compression stroke, but also part of the expansion stroke
109 [19]. The RCEM available at CMT-Motores Térmicos is a quasi-standard
110 experimental facility purchased by this laboratory, the results of which can
111 be compared directly with those from other RCEMs produced by the same
112 company.

113 A scheme of the RCEM is shown in Fig. 1. The RCEM is pneumatically
114 driven and its pistons are hydraulically coupled. As it can be seen, it can
115 be divided in two different zones, the experimentation zone and the driving
116 zone. The experimentation zone is composed by the combustion chamber.
117 The driving zone is composed by four different pistons. Piston 1, which is
118 called pushing piston, is pneumatically driven and hydraulically coupled to

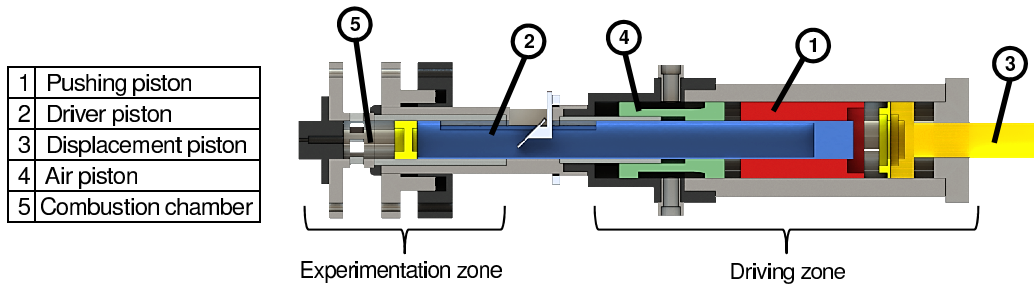


Figure 1: Rapid Compression Expansion Machine scheme.

119 piston 2, which is called driver piston and is directly connected with the
 120 combustion chamber. Piston 3 is hydraulically driven and it can be adjusted
 121 to select the compression stroke. Finally, piston 4 contains the compressed air
 122 that drives the machine. A detailed analysis about the operation principle
 123 of the RCEM can be found in Appendix A.

Bore	84	mm
Stroke	120 - 249	mm
Compression ratio	5 - 30	-
Maximum cylinder pressure	200	bar
Initial pressure	1 - 5	bar
Maximum heating temperature	393	K

Table 1: Technical characteristics of the RCEM.

124 The technical characteristics of the RCEM can be seen in Table 1. The
 125 pushing piston and the driver piston are instrumented with two AMO LMK102
 126 incremental position sensors, which allow knowing the absolute position of
 127 each piston with a resolution of 0.01 mm and, therefore, the combustion

128 chamber volume. The combustion chamber is composed by three elements,
129 the experimentation piston (mechanically connected to the driver piston),
130 the liner and the cylinder head. The experimentation piston consists on a
131 steel-made piston with 84 mm of bore and a quartz-made bowl with cylindri-
132 cal shape, 46 mm of bore and 17 mm of depth, which allow the axial optical
133 access. As the bowl is flat, the chamber can be recorded without any image
134 distortion. Moreover, three quartz-made windows with rectangular shape are
135 located in the liner to allow lateral optical access. Besides, the experimen-
136 tation piston is provided with an electrical 80 W heater that allows varying
137 the temperature of the bowl, and the cylinder head has four more electrical
138 heaters of 180 W each, which are responsible for heating the cylinder walls.
139 The walls temperature is measured by three thermoresistances PT1000 lo-
140 cated in the cylinder head, in the piston and in the bowl. The intake and
141 exhaust pipes are located in the liner of the combustion chamber. These
142 ducts are designed to induce swirl motion to the gases admitted by the ma-
143 chine. The turbulence generated during the filling is enough to guarantee
144 a homogeneous temperature in the chamber equal to the wall temperature,
145 as demonstrated by some previous CFD calculations. The cylinder head
146 is instrumented with a Kistler 6045A uncooled piezoelectric pressure sensor
147 with a sensitivity of -45 pC/bar, which is coupled to a Kistler 5018 charge
148 amplifier, and whereby the in-cylinder pressure is measured. Three Wika
149 piezoresistive pressure sensors are available to control the filling of the driv-
150 ing gas and of the combustion chamber with a resolution of 0.01 bar. The
151 injection system is a common rail system composed by a BOSCH solenoid-
152 commanded injector with a 7-hole nozzle and controlled by a EFS iPod power

153 driving module. This injection system has been characterized as explained
154 in [20].

155 The acquisition system is a Yokogawa DL850V composed by one 10 MHz-
156 12 bits module and five more 1 MHz-16 bits modules with two channels each.
157 The acquisition frequency is fixed to 10 MHz, which is necessary to capture
158 the pulses of the incremental position sensor. However, the in-cylinder pres-
159 sure and the injection pressure are recorded at 1 MHz.

160 The RCEM is filled from an external tank that can be heated up to
161 520 K thanks to three electrical heaters of 1200 W each. The synthetic air is
162 produced in the tank by a filling based on partial pressures where N₂, CO₂
163 and O₂ can be used. Besides, a syringe pump is available to allow the use of
164 H₂O. A vacuum pump is used to ensure the no contamination of the mixture
165 composition in this tank, nor in the RCEM charge. Finally, the synthetic
166 air is analyzed by gas chromatography in a Rapid Refinery Gas Analyser
167 from Bruker (450-GC) in order to know the exact composition and ensure
168 the correct reproduction of the experiments in CHEMKIN.

169 **3. Methodological approach**

170 A parametric study was carried out in a RCEM in order to analyze the
171 accuracy of a new method to predict ignition delays following this method-
172 ology: for a certain case, the evolutions of both the in-cylinder temperature
173 and pressure are experimentally obtained under motoring conditions. Then,
174 the ignition delay, τ , and the critical concentration, $[I]_{crit}$, are obtained for
175 each thermodynamic state by simulating in a perfectly stirred reactor. The
176 ignition delay under transient conditions is then predicted by using the new

177 procedure proposed in this paper and the Livengood & Wu integral method.
178 Besides, the ignition delay under transient conditions is obtained experimen-
179 tally and it is also calculated by simulating it in an internal combustion
180 engine reactor (direct chemical simulation) solving the detailed chemical ki-
181 netics mechanism. Finally, the values obtained for the ignition delay from
182 the direct chemical simulations are validated by comparing it with the ex-
183 perimental results, and the predicted ignition delays are compared directly
184 with these simulations. The comparison between the experimental results
185 and the predicted ignition delays is not possible since both are referred to
186 different stages of the autoignition process.

187 *3.1. New predictive method*

188 A new method to predict the ignition delay under transient thermody-
189 namic conditions is obtained starting from the Müller's model [21]. This new
190 procedure intends to improve the predictions obtained by the Livengood &
191 Wu integral by avoiding some of its hypotheses.

192 The low-temperature chain branching mechanism is the dominant one in
193 internal combustion engines (ICE) [22], since the evolution of the in-cylinder
194 temperature covers a wide range below 1000 K during the ignition delay.
195 Moreover, assuming that during the ignition delay the consumption of oxy-
196 gen is negligible, since the termination reactions are not very important, and
197 as $[O_2] \gg [F]$ and $[O_2] \gg [I]$ (where F represents the fuel and I repre-
198 sents the typical intermediates of the low-temperature fuel decomposition),
199 a constant oxygen concentration can be assumed. Considering an air-fuel
200 mixture under constant conditions of temperature and pressure the follow-
201 ing expression for the evolution of the concentration of chain carriers can be

202 obtained:

$$[I] = [I]_{crit} \frac{t}{\tau} \quad (2)$$

203 where $[I]_{crit}$ represents the critical concentration of chain carriers (maximum
204 concentration of chain carriers, which defines the ignition time).

205 If a process under transient conditions of pressure and temperature is
206 discretized as a series of thermodynamic states that remain constant for a
207 time dt , the ignition time can be obtained as follows:

$$1 = \frac{1}{[I]_{crit,t_i}} \int_0^{t_i} \frac{[I]_{crit}}{\tau} dt \quad (3)$$

208 where t_i is the ignition delay of the process and τ and $[I]_{crit}$ are the ignition
209 delay and the critical concentration of chain carriers under constant condi-
210 tions of pressure and temperature for the successive thermodynamic states.

211 It should be noted that if the critical concentration of chain carriers is
212 considered as a constant, Eq. 3 results in the Livengood & Wu integral.

213 The theoretical development performed to characterize the autoignition
214 phenomenon is described in detail in Appendix B.

215 3.2. RCEM

216 The desired stroke of the machine is selected and the RCEM is heated
217 up to the desired temperature. Two hours are needed in order to ensure a
218 homogeneous wall temperature. The synthetic air-EGR mixture is prepared
219 in the mixing tank. In this study, EGR was considered as the products of

220 a complete combustion reaction between the fuel and dry air in which the
221 amount of oxygen is the one desired by the user, as it is explained in [23].

222 Vacuum is created in the combustion chamber before the filling. The fuel
223 is injected into the combustion chamber at the start of the intake process
224 to avoid problems of stratification or other inhomogeneities. The turbulence
225 generated during the filling, as well as the long duration of the process (aprox-
226 imately 40 s), are enough to guarantee a homogeneous environment in the
227 chamber when the compression stroke starts.

228 The number of repetitions for each case to obtain a representative value
229 of the ignition delay have been selected by the following criterion: the semi-
230 amplitude of the confidence interval for the ignition delay with a level of
231 confidence of 95% may be higher than the 1% of the ignition delay average.
232 Thanks to the high repeatability of the machinen only five measurements are
233 needed for each case.

234 In this work the autoignition of the mixture is considered to be produced
235 when the time derivative of the pressure signal (which will be referred as
236 pressure rise rate or, simply, pressure rise further on) reaches a maximum.
237 Thus, the ignition delay in the experimental facility is defined as the time
238 between the start of the rapid compression process and the instant in which
239 the maximum pressure rise is obtained, as can be seen in Fig. 2.

240 Finally, the temperature profile is calculated for each experiment by ap-
241 plying the energy equation, since the pressure profile and the position of the
242 piston are known. The heat losses are characterized by a model based on the
243 Woschni correlation [24]. The calculation includes two additional models for
244 deformations and leaks, both of them explained in [25, 26].

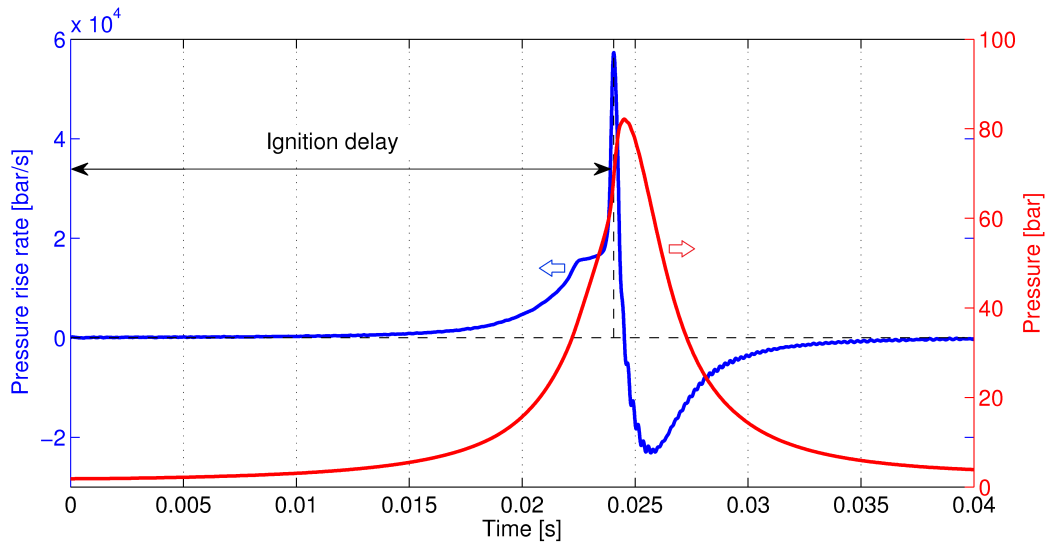


Figure 2: Ignition delay definition. The autoignition of the mixture is considered to be produced when the maximum pressure rise occurs.

245 3.3. CHEMKIN and chemical kinetic mechanisms

246 As mentioned before, CHEMKIN is the software used to obtain the
 247 different ignition delays and critical concentrations. The version used is
 248 CHEMKIN-PRO. Curran’s kinetic mechanism is used for n-heptane [27].
 249 This mechanism consists of 660 species and 2735 reactions and its validity
 250 has been checked in several articles [17, 28] by comparison with experimental
 251 results.

252 The model used to obtain ignition delays under constant conditions and
 253 critical concentrations is a homogeneous closed reactor (perfectly stirred reac-
 254 tor, PSR), which works with constant pressure and uses the energy equation
 255 to solve the temperature temporal evolution. This model is the most ap-
 256 propriate to obtain ignition delays under certain pressure and temperature

257 conditions [29]. Besides, working with constant pressure corrects, somewhat,
258 the over-prediction of the pressure which is typical of this kind of reactor
259 [30]. The autoignition of the mixture is considered to be produced when the
260 concentration of CH_2O reaches a maximum, since formaldehyde is widely
261 recognized as an autoignition tracer [31]. This means that when the criti-
262 cal concentration of formaldehyde is reached, the time corresponding to this
263 instant will be considered as the ignition delay. This criterion is the most
264 appropriate for the predictive methods, since they are based on it. Thus, a
265 criterion based on a critical concentration of chain carriers has to be used in
266 order to be consistent with the theoretical aspects of the predictive methods.
267 Any active radical with chain behavior can be taken as chain carrier, e. g.
268 HO_2 or H_2O_2 .

269 The model used to obtain ignition delays under transient conditions is a
270 reciprocating internal combustion engine operating with homogeneous charge
271 (IC-engine, closed 0-D reactors from CHEMKIN). The volume profile as well
272 as the heat loss profile are imposed in order to reproduce the RCEM condi-
273 tions. The piston starts at bottom dead center (BDC) and a complete cycle
274 of the RCEM is simulated. Two different criteria have be used to deter-
275 mine the ignition delay in this model. On the one hand, the autoignition is
276 considered to be produced when the time derivative of the pressure signal
277 reaches a maximum. This is the same criterion than the used in the ex-
278 periments and, therefore, it allows comparing the simulated results directly
279 with the experimental ones. On the other hand, the autoignition of the mix-
280 ture is considered to be produced when the concentration of CH_2O reaches
281 a maximum. Both criteria are used in the IC-engine model (direct chemical

282 simulations) in order to compare the simulation with both the experimental
283 and the predicted (Livengood & Wu and the new integral proposed) results.

284 It should be noted that whereas the experimental ignition delays are
285 based on a maximum pressure rise, ignition delays predicted by the numer-
286 ical methods are based on a maximum concentration of chain carriers (by
287 definition of the methods). Thus, ignition delays determined by both criteria
288 can differ because they are referred to different events of the autoignition
289 process.

290 Finally, the ignition delay, τ , and the critical concentration, $[I]_{crit}$, is ob-
291 tained for each thermodynamic state with a Δt of $5 \cdot 10^{-5} s$. The criterion
292 to select the working time step consists in choosing the one which relative
293 deviation in ignition delay is, at most, two times the deviation caused by a
294 time step. This means that the difference between the predicted and the sim-
295 ulated ignition delay should be lower than two time steps. This value of the
296 time step is chosen because it represents an equilibrium between appropriate
297 prediction accuracy and reasonable calculation time. Besides, the maximum
298 waiting time for the autoignition of the mixture has been set to 3 s, which
299 provides enough accuracy in the calculations.

300 3.4. Parametric study performed

301 The performed experimental study was as follows:

- 302 • Fuel: n-heptane.
- 303 • Initial temperature (T_0): 373 K and 383 K.
- 304 • Initial pressure (P_0): 0.134 MPa and 0.178 MPa.

- 305 • Compression stroke: 200 *mm* and 249 *mm*.
- 306 • Compression ratio (*CR*): 13, 15 and 17.
- 307 • Engine speed: 1000 *rpm*.
- 308 • Oxygen mass fraction (Y_{O_2}): 0.23, 0.16, 0.13 and 0.10.
- 309 • Equivalence ratio (*Fr*): from 0.27 to 1.45 depending on the oxygen
- 310 mass fraction.

311 The maximum equivalence ratio is limited by the working oxygen mass
 312 fraction in order to avoid extremely violent combustions. The performed
 313 parametric study can be seen in Table 2.

Y_{O_2}	<i>Fr</i>	Y_{O_2}	<i>Fr</i>	Y_{O_2}	<i>Fr</i>	Y_{O_2}	<i>Fr</i>
0.23	0.27	0.16	0.41	0.13	0.50	0.10	0.88
	0.34		0.50		0.60		1
	0.41		0.83		0.70		1.20
	0.50		0.88		0.88		1.45
	0.55						

Table 2: Parametric study performed.

314 Although equivalence ratios of 1.5 can seem uninteresting for practical
 315 applications, it must be taken into account that autoignition occurs under
 316 rich local equivalence ratios in direct-injection engines [32]. This concept is
 317 known as *most reactive mixture fraction* and it arises due to the balance
 318 of reactivities between the fuel-air ratio distribution and the temperature
 319 distribution.

320 4. Results and discussion

321 4.1. Comparison between experimental and direct chemical simulation results 322 (CHEMKIN)

323 Ignition delays obtained solving the n-heptane detailed chemical kinetic
324 mechanism are compared with the experimental results as a method to vali-
325 date the mechanism in the desired range.

326 As can be seen in Fig. 3 and Fig. 4, simulations reproduce with high
327 accuracy not only the trends, but also the values of the experimental results.
328 Ignition delay is defined in both cases as the time between the start of the
329 compression process and the instant in which the maximum pressure rise
330 occurs. As it is expected, the lower the oxygen mass fraction, the higher the
331 ignition delay (Fig. 3). Besides, Fig. 3 also shows that ignition delays decrease
332 when the compression ratio is increased, since the higher the compression
333 ratio the higher the reached temperatures. Finally, because the reaction
334 paths at low temperatures are dependant on radical species formed directly
335 from the fuel, the richer mixtures have lower ignition delays than the leaner
336 ones (Fig. 4).

337 The percentage deviation in ignition delay, ϵ , was calculated in order to
338 compare more easily experimental and simulation results. This deviation is
339 defined as follows:

$$\epsilon = \frac{t_{i,ICE} - t_{i,RCEM}}{t_{i,RCEM}} 100 \quad (4)$$

340 where t_i represents the time of ignition (ignition delay under transient con-
341 ditions). The subscript *ICE* represents a data obtained from a chemical

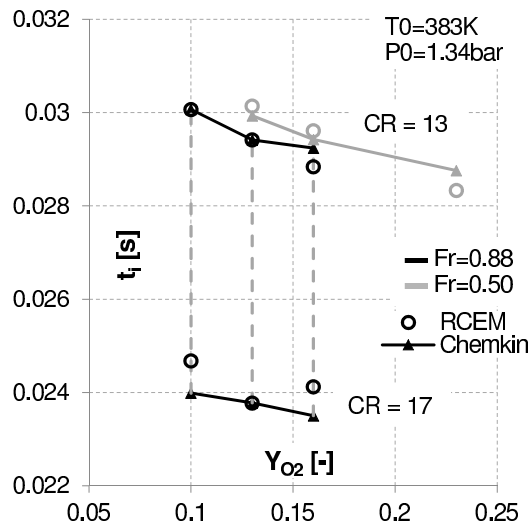


Figure 3: Ignition delay versus oxygen mass fraction at different equivalence ratios and compression ratios.

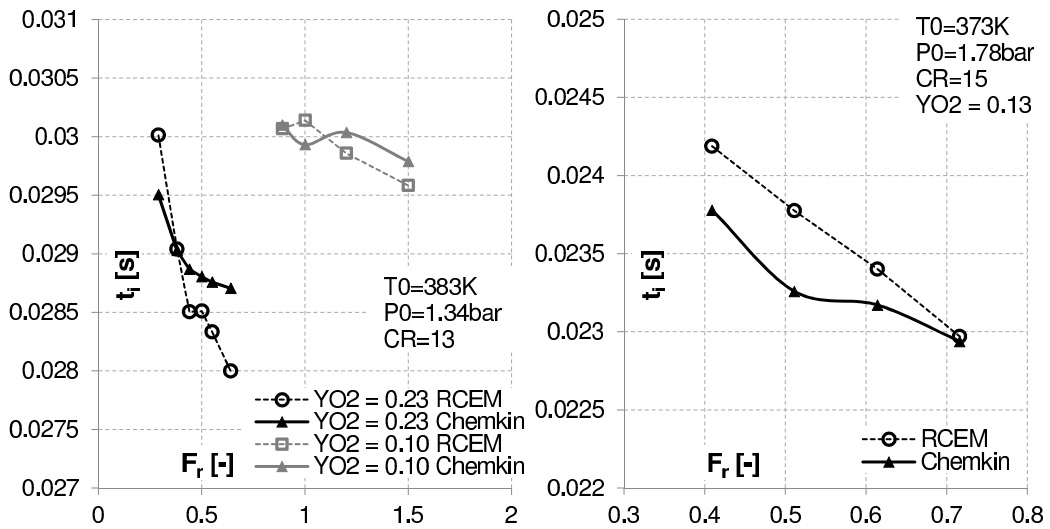


Figure 4: Ignition delay versus equivalence ratio at different oxygen mass fractions and compression ratios. Left.- Compression ratio = 13. Right.- Compression ratio = 15.

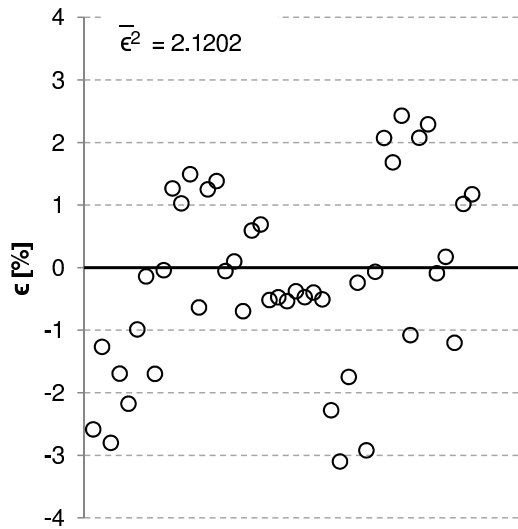


Figure 5: Percentage deviation in ignition delay. The mean square deviation, $\bar{\epsilon}^2$, shows a good agreement between both experimental and simulated results.

342 simulation with CHEMKIN using a closed 0-D IC-engine reactor. Finally,
 343 the subscript *RCEM* represents a data obtained experimentally from the
 344 RCEM.

345 The ignition delay deviation is shown in Fig. 5 for all cases. The mean
 346 square deviation, $\bar{\epsilon}^2$, has been calculated and its value can be seen in the
 347 figure.

348 The results show that simulations are able to reproduce the experimental
 349 ignition delays with quite good accuracy. In fact, the confidence interval for
 350 the mean square deviation, $\bar{\epsilon}^2$, with a confidence level of 95% is equal to
 351 [1.365, 2.875]. Ignition delay deviations are caused partly by the chemical
 352 kinetic mechanism used and partly by the uncertainties in the calculation of
 353 the effective volume and the heat losses of the RCEM.

354 *4.2. Comparison between the predictive methods and the direct chemical sim-*
355 *ulation*

356 Ignition delays under transient thermodynamic conditions are obtained
357 with the new proposed integral (Eq (3)), with the RCCC-method [33] and
358 with the Livengood & Wu integral method. The resulting predictions from
359 both methods are compared with the ignition delays obtained by the direct
360 chemical kinetic simulation.

361 It should be noted that whereas the experimental ignition delays are based
362 on a maximum pressure rise, $t_{i,dP2}$ (presented in Fig. 6, together with other
363 important events of the ignition process), which represents the high temper-
364 ature chemical stage, ignition delays predicted by the numerical methods are
365 based on a maximum concentration of chain carriers, t_{i,CH_2O} (by definition
366 of the methods). Thus, ignition delays determined by both criteria can differ
367 because they are referred to different events of the autoignition process as
368 can be seen in Fig. 6, where the normalized time derivative of pressure and
369 the normalized mole fraction of CH_2O are plotted for a certain case. The
370 most important events of a typical two-stage ignition are represented in the
371 figure, as well as various possible definitions for the ignition delay.

372 As can be seen in Fig. 7 and Fig. 8, ignition delays can be predicted
373 with high accuracy by the integral methods. Ignition delay is defined for all
374 simulations as the time between the start of the rapid compression process
375 and the instant in which the maximum concentration of CH_2O is reached,
376 t_{i,CH_2O} . Thus, the trends of the ignition delay change regarding the experi-
377 mental results, since the criterion to define this parameter is different.

378 The formation of CH_2O is controlled by the decomposition of the fuel to

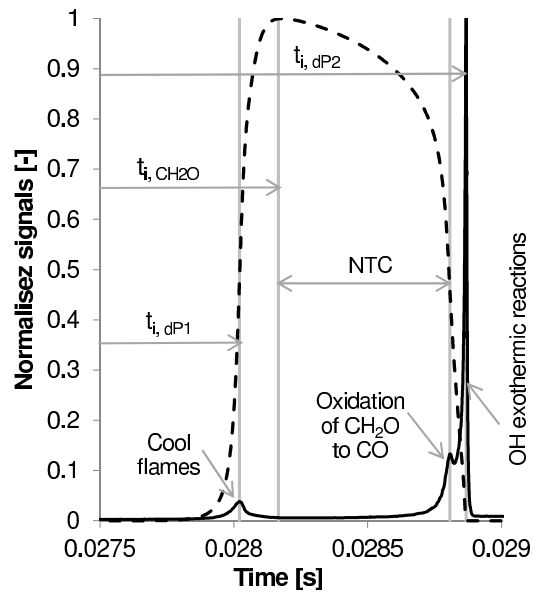


Figure 6: Important events of the ignition process and possible definitions of the ignition delay. The normalized time derivative of pressure (solid line) and the normalized mole fraction of CH_2O (dashed line) are plotted for a compression ratio of 13 and an initial temperature, pressure, equivalence ratio and oxygen mass fraction of 383 K, 1.34 bar, 0.50 and 0.23, respectively.

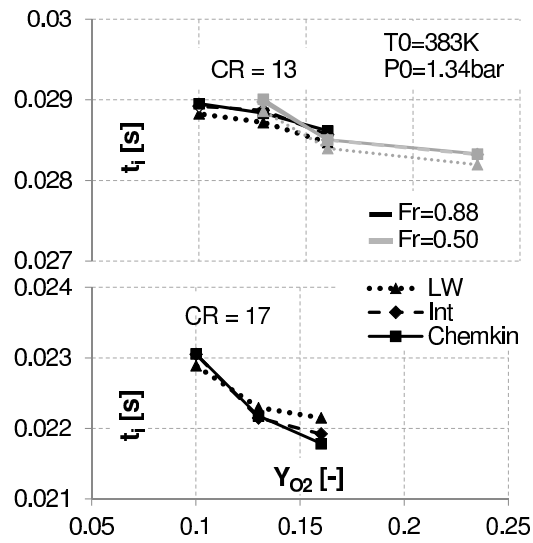


Figure 7: Ignition delay versus oxygen mass fraction at different equivalence ratios and compression ratios.

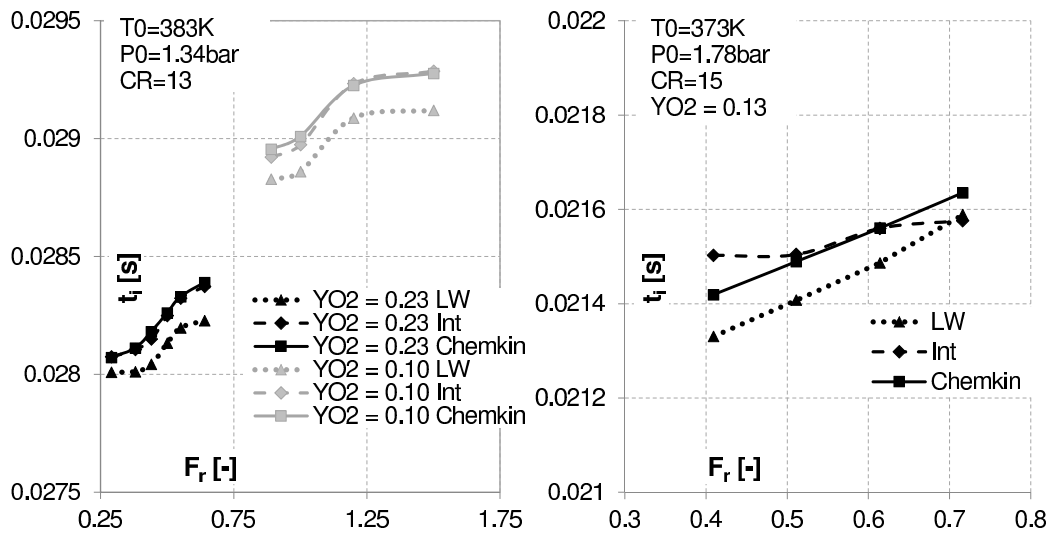


Figure 8: Ignition delay versus equivalence ratio at different oxygen mass fractions and compression ratios. Left.- Compression ratio = 13. Right.- Compression ratio = 15.

379 short chain hydrocarbons thanks to its combination with active radicals such
380 as HO_2 . These slight exothermic reactions cause the appearance of the cool
381 flames. Besides, the maximum heat release of the cool flames coincides with
382 the maximum generation rate of CH_2O .

383 Reactions that control the cool flames basically depend on temperature.
384 Moreover, the higher the equivalence ratio or the lower the oxygen mass
385 fraction, the higher the heat capacity of the gas mixture. Since a higher
386 heat capacity means higher heat sink effect, the mixture with a higher heat
387 capacity also undergoes (obviating chemical aspects) a slower temperature
388 increase. Thus, a richer or a more diluted mixture leads to later cool flames
389 and longer ignition delays $t_{i,dP1}$ and t_{i,CH_2O} (Fig. 7 and Fig. 8).

390 In the low-temperature chain branching mechanism, the decomposition
391 of CH_2O is controlled by the decomposition of H_2O_2 , which generates the
392 necessary OH radicals for oxidizing the formaldehyde to CO. The decompo-
393 sition of CH_2O define the transition between the NTC regime and the high
394 temperature branch. In fact, the disappearance rate of CH_2O depends on
395 the relevance of the NTC behavior. Besides, the NTC regime becomes less
396 pronounced if the pressure, the oxygen proportion or the equivalence ratio
397 are increased. Thus, a richer mixture or a less diluted mixture lead to a
398 faster decomposition of CH_2O and a shorter ignition delay $t_{i,dP2}$, as shown
399 in section 4.1.

400 It can be seen that the Livengood & Wu integral method underpredicts
401 the ignition delay with respect to the direct chemical simulation. This inte-
402 gral method assumes that the critical concentration is constant and equal to
403 the critical concentration at the ignition time. Since the critical concentra-

404 tion increases during the compression stroke of an engine, assuming it as a
405 constant leads to shorter ignition delays (the integral increases more rapidly).

406 The percentage deviation in ignition delay (or prediction deviation), ε ,
407 was calculated in order to compare more easily the prediction capability of
408 the methods. This deviation is defined as follows:

$$\varepsilon = \frac{t_{i,x} - t_{i,ICE}}{t_{i,ICE}} 100 \quad (5)$$

409 where t_i represents the time of ignition (ignition delay under transient con-
410 ditions). The subscript ICE represents a data obtained from a chemical
411 simulation with CHEMKIN using a closed 0-D IC-engine reactor. Finally,
412 the subscript x represents one of the predictive methods. The data obtained
413 from the Livengood & Wu numerical method are denoted by LW whereas
414 the predictions obtained from the new proposed integral (Eq (3)) are denoted
415 by Int .

416 The prediction deviation is shown in Fig. 9 in case of using both integral
417 methods and for all cases. The results show that the predictive methods
418 are able to reproduce the simulated ignition delays with high accuracy. The
419 mean square deviation, $\bar{\varepsilon}^2$, has been calculated for the two integral methods
420 and its value can be seen in the figure. In fact, the confidence interval for
421 the mean square deviation, $\bar{\varepsilon}^2$, with a confidence level of 95% is equal to
422 $[0.152, 1.238]$ for the Livengood & Wu integral method and to $[0, 0.178]$ for
423 the new integral proposed.

424 The results of the RCCC-method will only be shown in the form of confi-
425 dence intervals. They will not be presented in the different graphs for clarity
426 reason, since they are very close to those of the integral method proposed

427 here, and the different lines would not be distinguishable. The confidence
428 interval for the mean square deviation, $\bar{\varepsilon}^2$, with a confidence level of 95% is
429 equal to $[0, 0.093]$ for the RCCC-method, which is very similar to the one
430 obtained for the new integral proposed.

431 The new integral proposed by the authors in this paper takes into account
432 the dependence of the critical concentration with pressure and temperature,
433 discarding one of the hypotheses of the Livengood & Wu integral and leading
434 to more accurate predictions. However, this new integral method also as-
435 sumes that the autoignition process can be described by a zero-order global
436 reaction. This is the main difference with the RCCC-method, in which both
437 hypotheses are discarded at the expense of obtaining a numerical expression
438 much more complex than the integral methods.

439 The similitude in predicted ignition delays between both methods implies
440 that the generation rate of chain carriers during the ignition delay can be
441 assumed as a zero-order reaction. Moreover, it also implies that the improve-
442 ment in the predictions, comparing with the Livengood & Wu integral, are
443 caused almost in exclusive by the assumption of variable critical concentra-
444 tion.

445 There are some points for which the Livengood & Wu integral method
446 overpredicts the ignition delay and presents the highest prediction deviations.
447 In general, these points correspond also to the highest prediction deviations
448 for the new proposed integral method. In them, ignition occurs just in the
449 transition between the high and the low temperature mechanism. Fig. 10
450 shows the τ function for one of these cases. Despite the fact that the cal-
451 culations were carried out with a detailed chemical kinetic mechanism, the

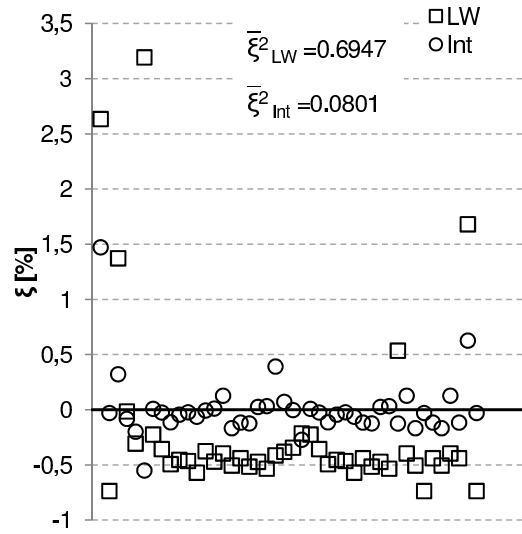


Figure 9: Percentage deviation in ignition delay. The mean square deviation, $\bar{\xi}^2$, shows a good agreement between both predicted and simulated results.

452 transition between the low temperature regime and the high temperature
 453 regime can result in discontinuities in τ . In these cases, discontinuities ap-
 454 pear in the interval in which the largest contribution to the integral is made,
 455 leading to higher prediction deviations. Moreover, these operating points
 456 also correspond to the highest deviations between the chemical simulations
 457 and the experimental results. According to the new integral method, this
 458 effect is not as dramatic as for the Livengood & Wu integral method since
 459 the variation of the critical concentration of chain carriers compensates the
 460 effect of the discontinuities in τ .

461 The Livengood & Wu method is also able to predict with quite accuracy
 462 ignition delays under transient conditions because the largest contribution
 463 to the integral is made in a narrow time range. This is the reason why the

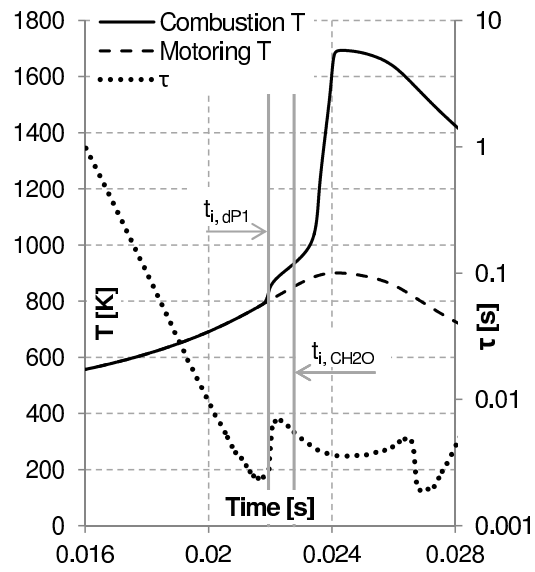


Figure 10: Combustion (solid line) and motoring (dashed line) temperatures and τ function (dotted line). The simulation has a compression ratio of 17 and an initial temperature, pressure, fuel/air equivalence ratio and oxygen mass fraction of 383 K, 1.34 bar, 0.60 and 0.13, respectively.

464 assumption of constant critical concentration does not invalidate the method
465 at all. Moreover, it can be checked that the critical concentration of chain
466 carriers decreases with temperature whereas it increases with pressure. The
467 relationship between pressure and temperature in an engine (simultaneous
468 increase or decrease of both) causes that the net variation of the critical
469 concentration is soft enough not to invalidate the Livengood & Wu integral
470 method, being the pressure effect dominant (the critical concentration of
471 chain carriers increases during the compression stroke and decreases during
472 the expansion stroke).

473 Finally, it should be noted that if the fuel does not present two-stage
474 ignition or if it presents a very smooth (or inexistent) NTC zone, the different
475 ignition delays are virtually the same and the predictive methods can be
476 compared directly with experimental results.

477 **5. Conclusions**

478 In this work a new method to predict ignition delays under transient
479 conditions from those obtained under constant conditions is developed. The
480 method is theoretically deduced from the Müller's mechanism, but it can
481 be obtained from other autoignition models following the same methodol-
482 ogy than the described in this paper, and it shows better results than the
483 Livengood & Wu integral method.

484 A detailed chemical kinetic mechanism has been validated in the working
485 range versus experimental results obtained from a RCEM. Then, the new
486 predictive method has been compared with the chemical simulations and
487 with the Livengood & Wu integral.

488 The following conclusions can be deduced from this study:

- 489 • The predictive methods presented in this paper are based on the premise
490 that autoignition occurs when the critical concentration of chain carriers
491 is reached. Therefore, the predicted ignition delays will be referred
492 to this criterion and the information used to obtain the predictions may
493 be also referred to this criterion.
- 494 • Care should be taken in comparing the predictions obtained from the
495 Livengood & Wu integral (and from the new integral method proposed)
496 with experimental results, since both ignition delays could be referred
497 to different stages of the combustion process.
- 498 • If the fuel does not present a two-stage combustion or if the NTC zone
499 is very soft, all criteria to define the ignition delay are virtually the
500 same and they can be compared with each other.
- 501 • If the autoignition occurs in the transition between the low and high
502 temperature chain branching mechanism, the chemical kinetic simula-
503 tion has shown the worst reproduction of the experimental results and
504 the integral methods have also shown the worst predictions. But, in
505 general, the detailed chemical kinetic mechanism is able to reproduce
506 the experimental data with high accuracy, as well as the predictive
507 methods are able to reproduce the chemical simulations.
- 508 • The trends of the ignition delay are different depending on the criterion
509 used to define it. Cool flames are strongly dependant on temperature.
510 Thus, the higher the equivalence ratio or the lower the compression

511 ratio and the oxygen content (higher EGR rate), the later the appear-
512 ance of the cool flames. Besides, the low-temperature chain branching
513 mechanism depends on radical species formed directly from the fuel.
514 Therefore, the higher the equivalence ratio, the earlier the maximum
515 pressure rise.

- 516 • A new method should be developed to predict ignition delays under
517 other criteria. Using the Livengood & Wu method to predict ignition
518 delays according to maximum pressure rise is not appropriate and can
519 lead to bad predictions.

520 **Acknowledgements**

521 The authors would like to thank different members of the CMT-Motores
522 Térmicos team of the Universitat Politècnica de València for their contribu-
523 tion to this work. The authors would also like to thank the member of ITQ,
524 Joaquín Martínez, for his help with the gas chromatography. The authors
525 are grateful to the Generalitat Valenciana for the financial support to acquire
526 the RCEM (references PPC/2013/011 and FEDER Operativo 2007/2013
527 F07010203PCI00CIMETUPV001). Finally, the authors would like to thank
528 the Spanish Ministry of Education for financing the PhD. Studies of Darío
529 López-Pintor (grant FPU13/02329). This work was partly founded by the
530 Generalitat Valenciana, project PROMETEOII/2014/043.k.

531 **Notation**

a_{st}	Oxygen-to-fuel ratio under stoichiometric conditions
BDC	Bottom Dead Center
CFD	Computational Fluid Dynamics
CI	Compression Ignition
CR	Compression Ratio
532 $crit$	Referred to the critical concentration
EGR	Exhaust Gas Recirculation
Fr	Working equivalence ratio
$HCCI$	Homogeneous Charge Compression Ignition
ICE	Referred to data obtained from CHEMKIN using the internal combustion engine reactor

<i>Int</i>	Referred to data obtained from the new integral proposed in this paper
k_i	Specific reaction rate of reaction i
<i>LW</i>	Referred to data obtained from the Livengood & Wu integral method
<i>LTC</i>	Low Temperature Combustion
<i>NTC</i>	Negative Temperature Coefficient
P_0	Initial pressure
<i>PCCI</i>	Premixed Charge Compression Ignition
<i>PRF</i>	Primary Reference Fuels
<i>PSR</i>	Perfectly Stirred Reactor
533 <i>SI</i>	Spark Ignition
T_0	Initial temperature
<i>TDC</i>	Top Dead Center
t_i	Ignition delay under transient conditions
t_{i,CH_2O}	Ignition delay referred to the critical concentration of CH_2O
$t_{i,dP1}$	Ignition delay referred to the maximum pressure rise of the cool flames
$t_{i,dP2}$	Ignition delay referred to the maximum pressure rise
<i>UHC</i>	Unburned hydrocarbons
Y_{O_2}	Oxygen mass fraction
ϵ	Percentage deviation in ignition delay between experimental and simulation results

	$\bar{\epsilon}^2$	Mean square deviation between experimental and simulation results
	ϵ	Ignition delay prediction deviation
534	$\bar{\epsilon}^2$	Mean square deviation of the predictive methods
	τ	Ignition delay under constant conditions of pressure and temperature

535 **Appendix A. Description and validation of the RCEM**

536 Rapid Compression Expansion Machines have the capability of replicat-
537 ing reasonably well the combustion process of reciprocating engines with fully
538 controlled initial and boundary conditions and avoiding the complexities as-
539 sociated to engines [34].

540 The RCEM available at CMT-Motores Térmicos has some important fea-
541 tures to perform various diagnostic studies under a wide range of experimen-
542 tal conditions: different compression ratios can be reached by varying the
543 stroke and the clearance volume, axial and lateral optical accesses are avail-
544 able [35, 36] and the compression velocity can be varied in order to simulate
545 different engine speeds. In a RCEM the expansion stroke of the piston can be
546 also analyzed and most of the engine parameters can be calculated under real
547 conditions, such as the heat release rate or the combustion efficiency. In this
548 facility both homogeneous and heterogeneous (direct injection) mixtures can
549 be tested, as well as new combustion modes such as the dual fuel technology
550 [37, 38] or LTC [39]. Of course, the RCEM allows the study of autoignition
551 of fuel-air mixtures under easily controlled and reproducible conditions in a

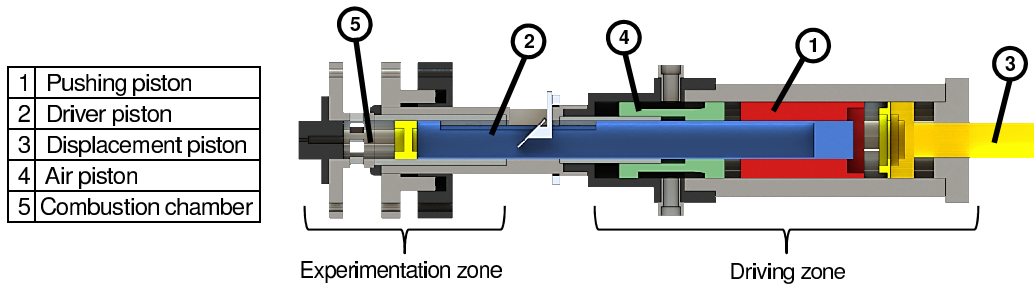


Figure A.11: Rapid Compression Expansion Machine scheme.

552 cleaner environment than in a traditional engine, without residual gases and
 553 with full control over the initial pressure and temperature, the volume and
 554 the trapped mass.

555 A scheme of the RCEM is shown in Fig. A.11. The RCEM is pneumati-
 556 cally driven and its pistons are hydraulically coupled. As it can be seen, it can
 557 be divided in two different zones, the experimentation zone and the driving
 558 zone. The experimentation zone is composed by the combustion chamber.
 559 The driving zone is composed by four different pistons. Piston 1, which is
 560 called pushing piston, is pneumatically driven and hydraulically coupled to
 561 piston 2, which is called driver piston and is directly connected with the
 562 combustion chamber. Piston 3 is hydraulically driven and it can be adjusted
 563 to select the compression stroke. Finally, piston 4 contains the compressed
 564 air that drives the machine.

565 First, the oil is pressurized by the driving gas, which is compressed air.
 566 The driver piston does not move because it is perfectly coupled to piston
 567 3, avoiding contact between the pushing oil and the piston base. Then,
 568 pressure is established behind the driver piston by a bypass valve and it

569 starts to advance at low velocity in a process called slow compression. It
570 should be noted that when the driver piston advances, the pushing piston
571 must advance also in the opposite direction, keeping constant the volume of
572 oil. In fact, both pistons are inertially balanced, leading to a process free of
573 vibrations.

574 When the driver piston leaves the piston 3, it is suddenly accelerated and
575 the rapid compression stroke starts. The driving air suffers an expansion
576 process whereby its pressure and, consequently, the pushing oil pressure, are
577 reduced. The piston stops when the pressure in the combustion chamber
578 is high enough to compensate the pushing force and the inertia, defining
579 TDC. Thereby, TDC is highly dependent on the operation conditions of the
580 RCEM, which is completely different for engines. Moreover, there is a certain
581 maximum driving pressure for each operating condition to avoid collision
582 of the piston with the cylinder head, since in the RCEM there is not any
583 mechanism as the rod-crank mechanism that fixes the maximum position of
584 the piston. Once the piston reaches TDC, the pressure in the combustion
585 chamber is higher than the pushing oil pressure and the expansion stroke
586 starts. More details on the operation principle of the RCEM can be found
587 in [40, 41].

588 This RCEM has been validated by comparison with the machine available
589 at ETH-Zurich, using the results showed in [36]. In that study, Mitakos et
590 al. studied the ignition delays referred to cool flames and referred to the
591 high temperature heat release of different fuels under various conditions of
592 temperature, equivalence ratio and EGR rate. The operating points of n-
593 heptane have been reproduced with the RCEM available at CMT-Motores

YO2	0.23		0.17		0.11	
Fr	0.42	0.3	0.56	0.4	0.86	0.6

Table A.3: Operating points of Mitakos et al. reproduced in the RCEM of CMT-Motores Térmicos

594 Térmicos and the results have been compared with the published ones.

595 The corresponding operating points can be seen in Table A.3, with an
596 initial temperature, pressure and stroke of 383 K, 1.34 bar and 249 mm.

597 In that case, the criterion to define the start of ignition delay is the time
598 at which the piston is at 200 mm. Besides, the start of ignition is considered
599 as the time at which the line that joins the 8% and the 25% of the maximum
600 heat release rate crosses by zero. Finally, the start of ignition referred to the
601 cool flames is considered as the time at which the line that joins the peak
602 and the 50% of the maximum heat release rate of cool flames crosses by zero.

603 It should be taken into account that the RCEM available at ETH is the
604 most similar to the one available at CMT. However, there are some construc-
605 tive differences between machines that cause a difference in the combustion
606 chamber volume and in some boundary conditions. Therefore, it is not pos-
607 sible to ensure the same pressure and temperature evolutions by reproducing
608 the same initial conditions and command settings.

609 In Fig. A.12 the correlation between both RCEMs can be analyzed. The
610 ignition delays obtained with the RCEM of CMT are plotted versus the ig-
611 nition delays obtained at ETH. The line $y = x$, which represents a perfect
612 match between values, has also been plotted in the figure. Finally, the co-
613 efficient of correlation R^2 has been calculated between both machines and

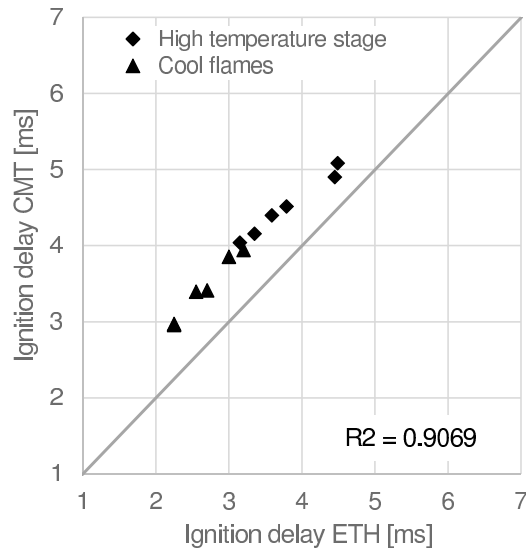


Figure A.12: Ignition delays obtained at CMT versus the corresponding values obtained at ETH. The coefficient of correlation between both machines has been calculated and its value is represented in the figure.

614 it is equal to 0.9069. As can be seen, the trends are perfectly reproduced
 615 at CMT. However, there is an offset between both results that is caused by
 616 the differences in dead volume and heat losses between machines. The fact
 617 that the differences in ignition delays are constant for all the experiments,
 618 which can be explained by constructive differences between RCEMs, allows
 619 the validation of the machine available at CMT-Motores Térmicos.

620 **Appendix B. Theoretical development of a new expression to pre-**
 621 **dict ignition delays**

622 The theoretical development performed to characterize the autoignition
 623 phenomenon is described in detail in this section. A new method to pre-

624 dict the ignition delay under transient thermodynamic conditions is obtained
 625 starting from the Müller’s model [21]. This new procedure intends to improve
 626 the predictions obtained by the Livengood & Wu integral by avoiding some
 627 of its hypotheses.

628 The Müller’s model is a simple model to characterize the autoignition
 629 phenomenon of the n-heptane by a chain reactions mechanism. It is com-
 630 posed by four reactions, which can be extended to any hydrocarbon C_nH_m
 631 as follows:



632 where a_{st} represents the oxygen-to-fuel molar ratio under stoichiomet-
 633 ric conditions, which is equal to $n + m/4$. Besides, F represents the fuel,
 634 Q represents the typical intermediates of the high-temperature fuel decom-
 635 position, I represents the typical intermediates of the low-temperature fuel
 636 decomposition, and P represents the main products of the combustion.

637 In this model, reactions R1 and R2 correspond to the high-temperature
 638 reaction branch, where R1 represents the high-temperature dehydrogenation
 639 and the thermal cracking of the fuel. Reactions R3 and R4 correspond to the

640 low-temperature chain branching mechanism. R3 is the chain reaction that
 641 promotes the progression of the autoignition process by the generation of
 642 chain carriers. Finally, R2 and R4 correspond to the termination reactions.
 643 The NTC behavior can be modeled by introducing a backward reaction in
 644 R3.

645 The low-temperature chain branching mechanism is the dominant one in
 646 internal combustion engines (ICE) [22], since the evolution of the in-cylinder
 647 temperature covers a wide range below 1000 K during the ignition delay.
 648 Thus, if ignition delays under ICE conditions want to be predicted, reactions
 649 R1 and R2 can be obviated. Under these hypotheses the species conservation
 650 equations can be written as follows:

$$\frac{d[F]}{dt} = -k_{3f}[F][O_2] + k_{3b}[I] \quad (\text{B.1})$$

$$\frac{d[I]}{dt} = k_{3f}[F][O_2] - k_{3b}[I] - k_4[I][O_2] \quad (\text{B.2})$$

$$\frac{d[O_2]}{dt} = a_{st} \frac{d[F]}{dt} + (a_{st} - 2) \frac{d[I]}{dt} \quad (\text{B.3})$$

651 where $[X]$ represents the concentration of the species X .

652 Moreover, assuming that during the ignition delay the consumption of
 653 oxygen is negligible, since the termination reactions are not very important,
 654 and as $[O_2] \gg [F]$ and $[O_2] \gg [I]$, a constant oxygen concentration can be
 655 assumed. Therefore, the previous conservation equations can be simplified
 656 as follows (Eq. B.4 is derived from Eq B.3, and Eq. B.5 from B.2 and B.4):

$$[F] = [F]_0 - \frac{a_{st} - 2}{a_{st}} [I] \quad (\text{B.4})$$

$$\frac{d[I]}{dt} = k_{3f}[O_2][F]_0 - \left(k_{3f} \frac{a_{st} - 2}{a_{st}} [O_2] + k_{3b} + k_4 [O_2] \right) [I] \quad (\text{B.5})$$

657 where $[F]_0$ is the initial fuel concentration.

658 Considering an air-fuel mixture under constant conditions of temperature
659 and pressure, the differential equation B.5 can be integrated with the initial
660 condition $t = 0 \rightarrow [I] = 0$ as follows:

$$1 - \frac{k_{3f} \frac{a_{st} - 2}{a_{st}} [O_2] + k_{3b} + k_4 [O_2]}{k_{3f} [O_2] [F]_0} [I] = \exp(-t(k_{3f} \frac{a_{st} - 2}{a_{st}} [O_2] + k_{3b} + k_4 [O_2])) \quad (\text{B.6})$$

661 where $\frac{1}{k_{3f} \frac{a_{st} - 2}{a_{st}} [O_2] + k_{3b} + k_4 [O_2]}$ is a characteristic time of the process and, there-
662 fore, it may be proportional to the ignition delay.

663 In order to simplify the expressions, the exponential term in Eq B.6 can
664 be approximated by a Taylor series expansion. The series can be truncated
665 in the second term, since $t(k_{3f} \frac{a_{st} - 2}{a_{st}} [O_2] + k_{3b} + k_4 [O_2]) \sim \frac{t}{\tau} < 1$ during the
666 ignition delay, and Eq B.6 can be rewritten as follows:

$$[I] = k_{3f} [O_2] [F]_0 t \quad (\text{B.7})$$

667 When $t = \tau$ the concentration of chain carriers is equal to the critical
668 concentration and the previous equation can be rewritten as follows:

$$[I] = [I]_{crit} \frac{t}{\tau} \quad (\text{B.8})$$

669 equation that is only valid under constant conditions of pressure and tem-
670 perature.

671 It should be noted that ignition represents a discontinuity in the model,
 672 since some hypotheses, as constant oxygen concentration, are no longer valid.
 673 In fact, the expression deducted for the generation rate of chain carriers loses
 674 its validity. Thus, although ignition happens when a maximum concentration
 675 of chain carriers occurs (the critical concentration), the generation rate of
 676 chain carriers predicted by the model at this instant is not equal to zero.

677 If a process under transient conditions of pressure and temperature is
 678 discretized as a series of thermodynamic states that remain constant for a
 679 time dt , the ignition time can be obtained as follows:

$$\int_0^{[I]_{crit,t_i}} d[I] = \int_0^{t_i} \frac{[I]_{crit}}{\tau} dt \rightarrow 1 = \frac{1}{[I]_{crit,t_i}} \int_0^{t_i} \frac{[I]_{crit}}{\tau} dt \quad (\text{B.9})$$

680 where t_i is the ignition delay of the process and τ and $[I]_{crit}$ are the ignition
 681 delay and the critical concentration of chain carriers under constant condi-
 682 tions of pressure and temperature for the successive thermodynamic states.

683 It should be noted that if the critical concentration of chain carriers is
 684 considered as a constant, Eq. B.9 results in the Livengood & Wu integral.

685 The new integral presented in this paper can be obtained by applying a
 686 similar theoretical development to different autoignition models, e. g. the
 687 Glassman's model [42]. In [33], the authors propose an alternative method
 688 to predict ignition delays under transient conditions, the RCCC-method.
 689 Whereas the Livengood & Wu integral assumes that the critical concentra-
 690 tion of chain carriers is constant and the production rate of active radicals
 691 can be assumed as a zero-order reaction, the new integral proposed in the
 692 present paper does not consider the critical concentration to be constant any-
 693 more, but still assumes a zero-order reaction for the chain carriers. Finally,

694 the RCCC-method discards both hypotheses, which might lead to a more
695 accurate method. However, the simplicity of the new integral proposed and
696 the small difference between the predictive accuracy of this method and the
697 RCCC-method make Eq. B.9 a very attractive method.

698 **References**

- 699 [1] U. Asad, J. Tjong, and M. Zheng. Exhaust gas recirculation - Zero
700 dimensional modelling and characterization for transient diesel combus-
701 tion control. *Energy Conversion and Management*, 86:309–324, 2014.
- 702 [2] T. Li, D. Wu, and M. Xu. Thermodynamic analysis of EGR effects on
703 the first and second law efficiencies of a boosted spark-ignited direct-
704 injection gasoline engine. *Energy Conversion and Management*, 70:130–
705 138, 2013.
- 706 [3] Z. Zheng, L. Yue, H. Liu, Y. Zhu, X. Zhong, and M-Yao. Effect of
707 two-stage injection on combustion and emissions under high EGR rate
708 on a diesel engine by fueling blends of diesel/gasoline, diesel/n-butanol,
709 diesel/gasoline/n-butanol and pure diesel. *Energy Conversion and Man-
710 agement*, 90:1–11, 2015.
- 711 [4] S.S. Nathan, J.M. Mallikarjuna, and A. Ramesh. An experimental study
712 of the biogas-diesel HCCI mode of engine operation. *Energy Conversion
713 and Management*, 51:1347–1353, 2010.
- 714 [5] K. Bahlouli, U. Atikol, R.K. Saray, and V. Mohammadi. A reduced
715 mechanism for predicting the ignition timing of a fuel blend of natural-

- 716 gas and n-heptane in HCCI engine. *Energy Conversion and Manage-*
717 *ment*, 79:85–96, 2014.
- 718 [6] J.C. Livengood and P.C. Wu. Correlation of autoignition phenomena in
719 internal combustion engines and rapid compression machines. *Sympo-*
720 *sium (International) on Combustion*, 5:347–356, 1955.
- 721 [7] L. Chen, T. Li, T. Yin, and B. Zheng. A predictive model for knock
722 onset in spark-ignition engines with cooled EGR. *Energy Conversion*
723 *and Management*, 87:946–955, 2014.
- 724 [8] M. Shahbakhti, R. Lupul, and C. R. Koch. Predicting HCCI auto-
725 ignition timing by extending a modified knock-integral method. *SAE*
726 *Paper no. 2007-01-0222*, 2007.
- 727 [9] Y. Ohyama. Engine control using a combustion model. *Seoul 2000*
728 *FISITA World Automotive Congress*, 2000.
- 729 [10] D.J. Rausen, A.G. Stefanopoulou, J.M. Kang, J.A. Eng, and T.W. Kuo.
730 A mean-value model for control of homogeneous charge compression
731 ignition HCCI engines. *Journal of Dynamic Systems, Measurement,*
732 *and Control*, 127:355–362, 2005.
- 733 [11] Y. Choi and J.Y. Chen. Fast prediction of start-of-combustion in HCCI
734 with combined artificial neural networks and ignition delay model. *Pro-*
735 *ceedings of the Combustion Institute*, 30:2711–2718, 2005.
- 736 [12] M. Hillion, J. Chauvin, and N. Petit. Control of highly diluted com-
737 bustion in diesel engines. *Control Engineering Practice*, 19:1274–1286,
738 2011.

- 739 [13] A.D.B. Yates, A. Swarts, and C.L. Viljoen. Correlating auto-ignition
740 delays and knock-limited spark-advance data for different types of fuel.
741 *SAE Paper no. 2005-01-2083*, 2005.
- 742 [14] L. Liang and R.D. Reitz. Spark ignition engine combustion modeling
743 using a level set method with detailed chemistry. *SAE Paper no. 2006-*
744 *01-0243*, 2006.
- 745 [15] R. Edenhofer, K. Lucka, and H. Kohne. Low temperature oxidation of
746 diesel-air mixtures at atmospheric pressure. *Proceedings of the Combustion*
747 *Institute*, 31:2947–2954, 2007.
- 748 [16] J.J. Hernandez, M. Lapuerta, and J. Sanz-Argent. Autoignition pre-
749 diction capability of the Livengood-Wu correlation applied to fuels of
750 commercial interest. *International Journal of Engine Research*, 15:817–
751 829, 2014.
- 752 [17] M. Sjoberg and J.E. Dec. An investigation into lowest acceptable com-
753 bustion temperatures for hydrocarbon fuel in HCCI engines. *Proceedings*
754 *of the Combustion Institute*, 30:2719–2726, 2005.
- 755 [18] D. Mitakos, C. Blomberg, Y. Wright, P. Obrecht, B. Schneider, and
756 K. Boulouchos. Integration of a cool-flame heat release rate model into
757 a 3-stage ignition model for HCCI applications and different fuels. *SAE*
758 *Paper no. 2014-01-1268*, 2014.
- 759 [19] G. Barroso, A. Escher, and K. Boulouchos. Experimental and numerical
760 investigations on HCCI combustion. *SAE Paper no. 2005-24-038*, 2005.

- 761 [20] R. Payri, F.J. Salvador, J. Gimeno, and G. Bracho. A new methodol-
762 ogy for correcting the signal cumulative phenomenon on injection rate
763 measurements. *Experimental Techniques*, 32:46–49, 2008.
- 764 [21] N. Peters U.C. Müller and A. Liñán. Global kinetics for n-heptane
765 ignition at high pressures. *Twenty-Fourth Symposium (International)*
766 *on Combustion*, pages 777–784, 1992.
- 767 [22] X.C. Lu, W. Chen, and Z. Huang. A fundamental study on the control
768 of the HCCI combustion and emissions by fuel design concept combined
769 with controllable EGR. Part 1. The basic characteristics of HCCI com-
770 bustion. *Fuel*, 84:1074–1083, 2005.
- 771 [23] J. M. Desantes, J. J. López, S. Molina, and D. López-Pintor. Design
772 of synthetic EGR and simulation study of the effect of simplified for-
773 mulations on the ignition delay of isooctane and n-heptane. *Energy*
774 *Conversion and Management*, 96:521–531, 2015.
- 775 [24] G. Woschni. A universally applicable equation for the instantaneous
776 heat transfer coefficient in the internal combustion engine. *SAE Paper*
777 *no. 670931*, 1967.
- 778 [25] J. Benajes, P. Olmeda, J. Martín, and R. Carreño. A new methodology
779 for uncertainties characterization in combustion diagnosis and thermo-
780 dynamic modelling. *Applied Thermal Engineering*, 71:389–399, 2014.
- 781 [26] F. Payri, S. Molina, J. Martín, and O. Armas. Influence of measure-
782 ment errors and estimated parameters on combustion diagnosis. *Applied*
783 *Thermal Engineering*, 26:226–236, 2006.

- 784 [27] H.J. Curran, P. Gaffuri, Pitz W.J, and C.K. Westbrook. A comprehensive
785 modeling study of n-heptane oxidation. *Combustion and Flame*,
786 114:149–177, 1998.
- 787 [28] H.J. Curran, W.J. Pitz, C.K. Westbrook, C.V. Callahan, and F.L. Dryer.
788 Oxidation of automotive primary reference fuels at elevated pressures.
789 *Proceedings of the Combustion Institute*, 27:379–387, 1998.
- 790 [29] F. Payri, X. Margot, S. Patouna, F. Ravet, and M. Funk. Use of a
791 single-zone thermodynamic model with detailed chemistry to study a
792 natural gas fueled Homogeneous Charge Compression Ignition engine.
793 *Energy Conversion and Management*, 53:298–304, 2012.
- 794 [30] P. Redón. *Modelling of the nitrogen oxides formation process applicable*
795 *to several diesel combustion modes*. PhD thesis, Universitat Politècnica
796 de València, Valencia (Spain), 2013.
- 797 [31] B. Baeuerle, J. Warnatz, , and F. Behrendt. Time-resolved investigation
798 of hot spots in the end gas of an S.I. engine by means of 2-D double-
799 pulse LIF of formaldehyde. *Symposium (International) on Combustion*,
800 2:2619–26256, 1996.
- 801 [32] E. Mastorakos. Ignition of turbulent non-premixed flames. *Progress in*
802 *Energy and Combustion Science*, 35:57–97, 2009.
- 803 [33] J. M. Desantes, J. J. López, S. Molina, and D. López-Pintor. Validity
804 of the Livengood & Wu correlation and theoretical development of an
805 alternative procedure to predict ignition delays under variable thermo-
806 dynamic conditions. *Energy Conversion and Management*, 0:0–1, 2015.

- 807 [34] A. C. Scardini Villela, S. Leal Braga, J. C. Cuisano Egúsquiza, and
808 G. Bastos Machado. Rapid compression machine tests for brazilian otto
809 cycle fuels. *SAE Paper no. 2011-36-0349*, 2011.
- 810 [35] S. Manasra and D. Brueggemann. Effect of injection pressure and timing
811 on the in-cylinder soot formation characteristics of low CR neat GTL-
812 Fueled DI diesel engine. *SAE Paper no. 2011-01-2464*, 2011.
- 813 [36] D. Mitakos, C. Blomberg, A. Vandersickel, Y. Wright, B. Schneider,
814 and K. Boulouchos. Ignition delays of different homogeneous fuel-air
815 mixtures in a Rapid Compression Expansion Machine and comparison
816 with a 3-stage-ignition model parametrized on shock tube data. *SAE*
817 *Paper no. 2013-01-2625*, 2013.
- 818 [37] J. C. Cuisano Egúsquiza, S. Leal Braga, C. V. Maciel Braga, A. C. Scar-
819 dini Villela, and N. Reis de Moura. Experimental investigation of the
820 natural gas / diesel dual-fuel combustion using a Rapid Compression
821 Machine. *SAE Paper no. 2011-36-0360*, 2011.
- 822 [38] S. Schlatter, B. Schneider, Y. Wright, and K. Boulouchos. Compara-
823 tive study of ignition systems for lean burn gas engines in an optically
824 accessible Rapid Compression Expansion Machine. *SAE Paper no. 2013-*
825 *24-0112*, 2013.
- 826 [39] T. Steinhilber and T. Sattelmayer. The effect of water addition on HCCI
827 diesel combustion. *SAE Paper no. 2006-01-3321*, 2006.
- 828 [40] S. Schlatter, B. Schneider, Y. Wright, and K. Boulouchos. Experimental
829 study of ignition and combustion characteristics of a diesel pilot spray

- 830 in a lean premixed methane/air charge using a Rapid Compression Ex-
831 pansion Machine. *SAE Paper no. 2012-01-0825*, 2012.
- 832 [41] M. Pöschl and T. Sattelmayer. Influence of temperature inhomogeneities
833 on knocking combustion. *Combustion and Flame*, 153:562–573, 2008.
- 834 [42] I. Glassman and R.A. Yetter. *Combustion*. Elsevier Academic Press,
835 2008.